A geometric-based convection approach of 3-D reconstruction

Raphaëlle Chaine

A geometric-based convection approach of 3-D reconstruction

Raphaëlle Chaine

N° 4688

Décembre 2002

THÈME 2

Rapport de recherche

A geometric-based convection approach of 3-D reconstruction

Raphaëlle Chaine*

Abstract: Surface reconstruction algorithms produce piece-wise linear approximations of a surface S from a finite, sufficiently dense, subset of its points. In this paper, we present a fast algorithm for surface reconstruction from scattered data sets. This algorithm is inspired of an existing numerical convection scheme developed by Zhao, Osher and Fedkiw. Unlike this latter, the result of our algorithm does not depend on the precision of a (rectangular) grid. The reconstructed surface is simply a set of oriented faces located into the 3D Delaunay triangulation of the points. It is the result of the evolution of an oriented pseudo-surface. The representation of the evolving *pseudo*-surface uses an appropriate data structure together with operations that allow deformation and topological changes of it. The presented algorithm can handle complicated topologies and, unlike most of the others schemes, it involves no heuristic. The complexity of that method is that of the 3D Delaunay triangulation of the points. We present results of this algorithm which turned out to be efficient even in presence of noise.

Key-words: 3D reconstruction, surface convection, computational geometry, geometrical and topological operations, Delaunay triangulation

Une approche de la reconstruction 3D par convection géométrique

Résumé : Etant donné un ensemble suffisamment dense de points 3D échantillonnés sur une surface, les algorithmes de reconstruction 3D permettent d'obtenir une approximation linéaire par morceaux de cette surface. Dans cet article, nous présentons un algorithme rapide et robuste de reconstruction 3D. Cet algorithme est inspiré d'un modèle numérique de convection développé par Zhao, Osher et Fedkiw, mais il s'affranchit de la nécessité d'utiliser une grille. Ainsi la qualité du résultat ne dépend plus de la précision d'une telle grille. La surface reconstruite se présente sous forme d'un ensemble de facettes triangulaires orientées, extraites de la triangulation de Delaunay de l'ensemble des points. Ces facettes résultent de l´évolution d'une *pseudo*-surface orientée. La déformation de cette *pseudo*-surface nécessite l'utilisation d'une structure de donnée adaptée, ainsi qu'un jeu d'opérations géométriques et topologiques qui permettent de la faire évoluer. L'algorithme présenté permet de traiter la reconstruction d'objets de topologie complexe, même en présence de données bruitées. A la différence de la plupart des méthodes existantes, cet algorithme ne s'appuie sur aucune heuristique. Sa complexité se ramène à celle de la construction de la triangulation de Delaunay. Nous présentons quelques résultats obtenus grâce à cet algorithme.

Mots-clés : reconstruction 3D, convection de surface, géométrie algorithmique, évolution géométrique et topologique, structures de données, triangulation de Delaunay

1 Introduction : the reconstruction problem

Given a set of points that lie on or near an object surface, we consider the problem of computing a piecewise linear approximation of this unknown surface. The reconstruction problem has received considerable attention both in computer graphics and computational geometry. In computer graphics, the early work by Hoppe *et al* [1] proposes an implicit approximation of the surface to be reconstructed. Curless and Levoy [2] have presented a similar approach dedicated to range images. The works by Bernardini *et al* [3] and Gopi *et al* [4] are closer to computational geometry approaches which are more combinatorial. They output a set of facets from geometric data structures such as the Delaunay triangulation of the points. Early works of reconstruction in computational geometry are the α-shapes of Edelsbrunner [5] and the sculpture algorithm by Boissonnat [6]. Later on, Amenta and Bern [7] have proposed the first algorithm with correctness guarantees under a given sampling condition (CRUST). An improved version of this algorithm (COCONE) [8] has also been described. Some existing algorithms do not necessarily extract the reconstructed surface from the 3D Delaunay triangulation of the points. For example, the POWER-CRUST of Amenta et al [9] uses a power-diagram of the points. As far as Boissonnat and Cazals [10] are concerned, they use the Voronoi diagram of the points to produce an implicit version of the surface. Eventually, recent approaches of Giesen and John [11] and Edelsbrunner [12] introduce the notion of flow in computational geometry. The work presented in this paper is of that kind.

Contents. (2) Convection model, (2.1) Convection model proposed by Zhao, Osher and Fedkiw, (2.2) Fast tagging algorithm, (3) Convection and computational geometry, (3.1) Geometric properties, (3.2) Convection result through a geometric algorithm, (3.3) Oriented nature of the aperture condition, (4) Extension of the convection process, (5) Topological structure of the result, (5.1) Geometrical and topological operations involved during the convection process, (6) Results, (7) Conclusion.

2 Convection model

2.1 Convection model proposed by Zhao, Osher and Fedkiw

In [13], Zhao, Osher and Fedkiw propose a function E to measure the distance between a surface Γ and a set of points Σ. This global distance or energy can be seen as a weighted area of the surface, where each surface element is weighted by its distance to its closest point in the data set Σ.

$$E(\Gamma) = \left(\int_{x \in \Gamma} d^p(x) \, ds \right)^{1/p} 1 \leq p \leq \infty$$

where $d(x)$ is the distance from $x \in I\!\!R^3$ to its closest point in Σ.

Once this functional energy defined, Zhao, Osher and Fedkiw suggest to solve the reconstruction problem as the one of determining a surface which minimizes the global distance

function to the data set Σ. They propose a variational formulation and an evolution equation to construct this minimal surface by deformation of a good initial enclosing approximation of the surface. More details on the way they extend this model to implicit level set surfaces can be found in [13].

The evolution runs a gradient descent of the energy functional to be minimized. At each step, each point x of the surface evolves along its normal direction, towards the interior of the surface, with a displacement speed proportional to $-\nabla d(x).n + (d(x)K)/p$ where K is the mean curvature of the surface and n the inner unit normal at point x. The tension of the surface represented by the second term is non linear so that the evolution requires a huge quantity of steps before reaching its equilibrium.

The better the initial approximation of the surface is, the more the non linear effect of the evolution model is counteracted. In this paper, we want to focus on the convection model Zhao, Osher and Fedkiw use to construct a good initial approximation of the surface. It is a simple, physically motivated, convection model that they solve with a so-called "fast tagging algorithm".

Given a flexible enclosing surface Γ, Zhao, Osher and Fedkiw put it into a velocity field $-\nabla d(x)$ created at point x by the distance function to the data set. In this velocity field, points of a curve or a surface are attracted towards their closest point in the data set, except the points located at an equal distance from two or more data points. In the model they consider, the surface is also subject to viscosity, so that it does not split into points : during its evolution, each point of the surface is always moved along its normal direction with a displacement speed $-\nabla d(x).n$. At the equilibrium, the evolving curve (resp. surface) reaches a polygon (resp. a polyhedron), the vertices of which belong to the data set as the viscosity tends to zero. Each point of this resulting surface also satisfies the steady state equation : $\nabla d(x).n = 0$

2.2   Fast tagging algorithm

The "fast tagging algorithm" [13] is a fast numerical scheme that identifies the interior from the exterior of the convection resulting surface. This algorithm requires the distance function $d(x)$ to be known at each point of a regular grid (Zhao et al solve it by an upwind difference scheme in $O(n + N)$ for n data points and N grid points).

Once the distance d has been calculated everywhere, each point of the grid is tagged as interior or exterior : starting from a bounding connected set of points tagged as exterior (the points of a bounding box), a heap sort is built with the set of tagged exterior points that are adjacent to an untagged point.

Let x be the point of the heap with the largest d value (x is popped) :

- If at least one untagged neighbor of x has a larger d value, x is tagged as a boundary point.

- If all untagged neighbors of x have smaller d value than x has, they are tagged as exterior and pushed into the heap sort.
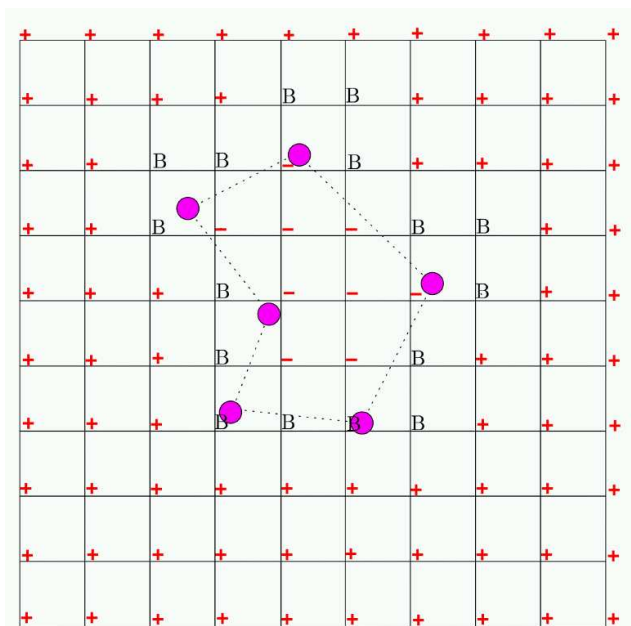
Figure 1: "Fast tagging algorithm" : exterior points are tagged as $+$, interior points are tagged as $-$, boundary points are tagged as B

Fig. 1 illustrates the result of the "fast tagging algorithm" in 2D. Zhao et al show that this algorithm converges and has a complexity $O(NlogN)$.

The "fast tagging algorithm" is a numerical scheme that is clearly driven by the geometry. In this paper, we present a geometric algorithm in order to produce the same result without using a grid.

Related work has begun to appear in the computational geometry community. In year 2002, Giesen et al [11] have proposed a general study of the repulsion field $\nabla d(x)$, together with a reconstruction algorithm based on cells composed of points having the same attractor. A similar idea to the one presented in our paper has also been used in the software *Geomagic Wrap* developed by Herbert Edelsbrunner [12]. That work has been subject to a 5 years long patent and has not been published yet. The reconstruction approach presented in our paper has been developed independently and is based an a different formalism.

3   Convection and computational geometry

3.1   Geometric properties

In this part, we show that the result of the convection model proposed by Zhao, Osher and Fedkiw is a triangulated oriented surface that is included into the 3D Delaunay triangulation of the set of points. We also prove that each oriented facet of the result meet a particular geometric property.

There is an equivalent of this result in the 2D case of convection towards a set of points in $I\!\!R^2$. We first present this simpler case to make a comprehensive step towards the 3D case.

Definition 1

- *Edge : 1-simplex defined by a set of 2 points in $I\!\!R^2$.*

- *Half-edge : there are 2 possible orientations of an edge. An oriented edge is called a half-edge. Given 2 points P_1 and P_2, $\overset{\frown}{P_1 P_2}$ denotes the half-edge supported by P_1 and P_2, oriented from P_1 to P_2. An edge can be seen as the union of 2 half-edges.*

- *Given an edge e, the diametral disk of e can be seen as the union of 2 half-disks respectively supported by the two associated half-edges. The half-disk associated to a half-edge $\overset{\frown}{P_1 P_2}$ is located on its left hand (see fig. 2).*

- *Given a set of 2D points, an edge (resp. a half-edge) is said to meet the Gabriel property if its associated disk (resp. half-disk) does not contain any point of the set.*
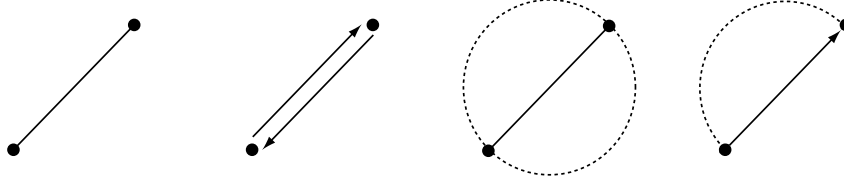

Figure 2: *a)* edge, *b)* edge as the union of 2 half-edges, *c)* disk associated to an edge, *d)* half-disk associated to a half-edge

Similar definitions are available in $I\!\!R^3$:

Definition 2

- *Facet : 2-simplex defined by a set of 3 points in $I\!\!R^3$*

- *Half-facet : There are 2 possible orientations of a facet. An oriented facet is called a half-facet. Given 3 points P_1, P_2 and P_3, $\overset{\frown}{P_1 P_2 P_3}$ denotes the half-facet supported by P_1, P_2 and P_3, the orientation of which is given by $\overrightarrow{P_1 P_2} \wedge \overrightarrow{P_1 P_3}$. A facet can be seen as the union of 2 half-facets. These 2 half-facets are said to be coupled.*

- *Given a facet f, the diametral ball of f can be seen as the union of 2 half-balls respectively supported by the two associated half-facets.*

- *Given a set of 3D points, a facet (resp. a half-facet) is said to meet the Gabriel property, if its associated ball (resp. half-ball) does not contain any point of the set.*

Lemma 3 *Given a set Σ of points in $\mathbb{R}^2$, the result of the convection of a bounding curve towards Σ is a closed oriented pseudo-curve composed of a set of half-edges. These half-edges are oriented towards the interior of the curve, they are supported by edges of the 2D Delaunay triangulation of Σ and they all meet the Gabriel property. The term pseudo-curve is used to mean that different parts of the evolving curve can locally meet common geometric information.*

Proof. Let C be an initial bounding curve oriented towards the data. C can be split into pieces, so that each piece of C intersects $d = 2$ neighboring Voronoi cells only, to the exclusion of any other Voronoi cell (see Fig. 3).
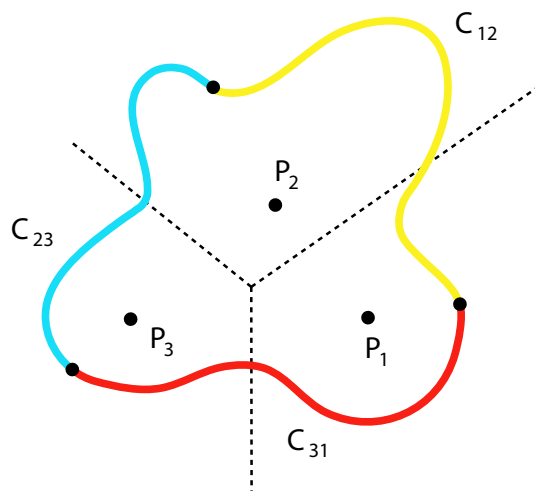

Figure 3: Split of C into pieces going through $d = 2$ adjacent Voronoi cells only

Let C_{ij} be the piece of curve intersecting the adjacent Voronoi cells of $d = 2$ points P_i and P_j, oriented accordingly to the half-edge $\overset{\frown}{P_i P_j}$ (see Fig. 4). Since the Voronoi cells of P_i and P_j are adjacent, the $(d-1)$-simplex $P_i P_j$ is included into the Delaunay triangulation of the points.

We consider the result of the convection of C_{ij} towards Σ.

Along $\nabla d(x)$, the points of C_{ij} located inside the Voronoi cell of P_i are attracted towards P_i, whereas the points located inside the Voronoi cell of P_j are attracted towards P_j. The
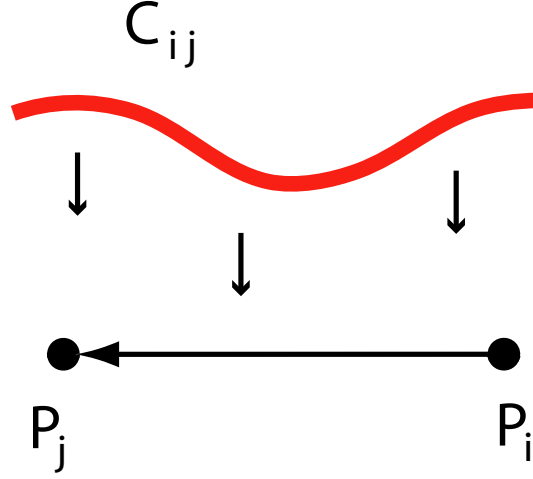
Figure 4: Consistent orientation between C_{ij} and $\overset{\frown}{P_iP_j}$

points equidistant of P_i and P_j are attracted towards the middle of $[P_iP_j]$. Here, *towards* does not mean that moving points will end into their (local) attractor. During its evolution, the attractor of one point can change. Moreover, points of C_{ij} do not evolve any more when all of them meet $\nabla d(x).n = 0$ (viscosity effect).

First case :   The half-edge $\overset{\frown}{P_iP_j}$ does not meet the Gabriel property. It means that the half-disk associated to $\overset{\frown}{P_iP_j}$ contains at least another point of the set. P_iP_j is included into the Delaunay triangulation of the points. Let P_k be the point which is also connected to P_i and P_j in the Delaunay triangulation and that lies in the half-plane delimited by $\overset{\frown}{P_iP_j}$ (We say that P_k is the point *hidden by* $\overset{\frown}{P_iP_j}$). P_k is one of the points included into the half-disk associated to the half-edge P_iP_j (consider the pencil of circles going through P_i and P_j).

The Voronoi center of P_i, P_j and P_k is not located into the half-plane delimited by the half-edge $\overset{\frown}{P_iP_j}$, which means that points of C_{ij} meet the Voronoi cell of P_k on their way to their attractor.

At this state of its evolution, C_{ij} can be split into $d = 2$ pieces C_{ik} and C_{kj} respectively intersecting the adjacent Voronoi cells of P_i and P_k for C_{ik}, and P_k and P_j for C_{kj}. The result of the evolution of C_{ij} is the result of the evolution of C_{ik} and C_{kj}. $\overset{\frown}{P_iP_k}$ and $\overset{\frown}{P_kP_j}$ are said to be the half-edges hidden by $\overset{\frown}{P_iP_j}$.

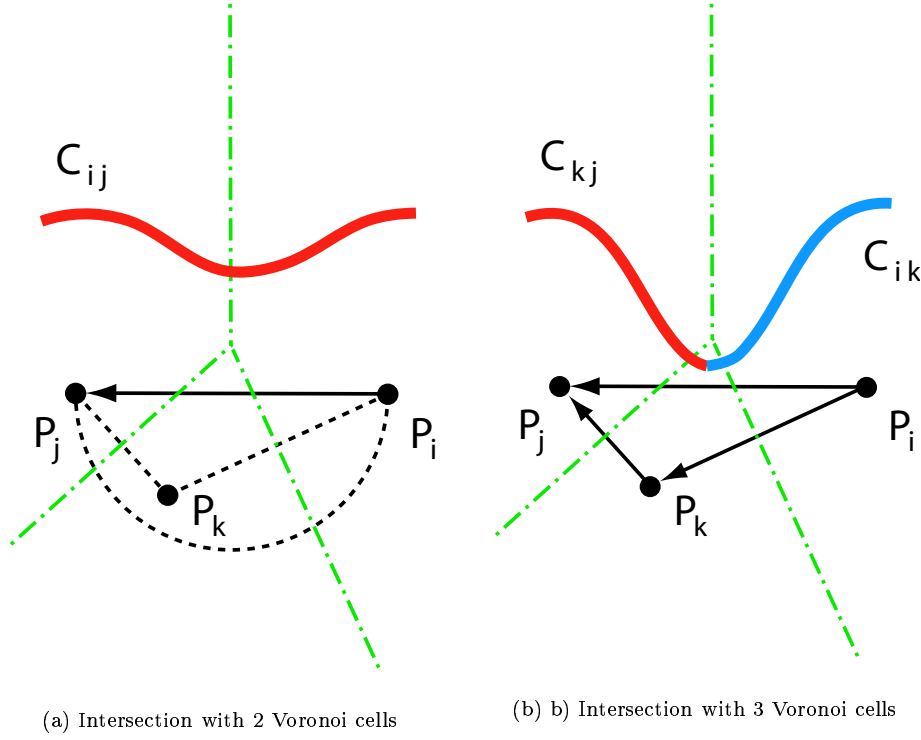(a) Intersection with 2 Voronoi cells   (b) b) Intersection with 3 Voronoi cells

Figure 5: Attraction towards a half-edge without the Gabriel property

Second case : The half-edge $\overset{\frown}{P_i P_j}$ meets the Gabriel property. In that case, no new Voronoi cell is encountered by the points of C_{ij} on their way to their attractor. The points of the surface are attracted by their closest point in the set and are dragged by their neighbors so that the result of the convection of C_{ij} is the entire half-edge $\overset{\frown}{P_i P_j}$, supported by an edge of the Delaunay triangulation.

Termination : Previous analysis has dealt with local evolution of the curve. We are left with the case of auto-intersection at different parts of the curve during the convection scheme.

If ever the curve was to intersect itself apart two coupled half-edges, it would collapse in this area with a possible creation of a hole and a possible change in the genus of the evolving closed curve. We show in Section 5, that this does not happen in the case of a 2D convection. It can happen however in the 3D case.

At each step, the curve shrinks towards its interior, so that the positive area it encloses decreases. This ensures the termination of the convection scheme.   □

A similar result with a similar demonstration holds in 3D :

Lemma 4 *Given a set Σ of points in $\mathrm{I\!R}^3$, the result of the convection of a bounding surface towards Σ is a closed oriented pseudo-surface composed of a set of half-facets. These half-facets are oriented towards the interior of the surface. They are supported by facets of the Delaunay triangulation of Σ and they all meet the Gabriel property. The term pseudo-surface is used in the sense that different parts of the evolving surface can locally meet common geometric information.*

3.2   Convection result through a geometric algorithm

A geometric algorithm computing the convection result of an enclosing surface can be derived easily from the previous results. Such an algorithm consists in making a triangulated oriented surface shrink into the 3D Delaunay triangulation of the points until it locally fits Σ with half-facets verifying the Gabriel property.

The evolving surface is initialized with the set of half-facets that are lying on the convex-hull of Σ and that are oriented towards its interior.

The oriented surface evolves, subject to geometric and topological operations that will be described in detail in Section 5. This deformation scheme can be described as follows (see Fig. 6).
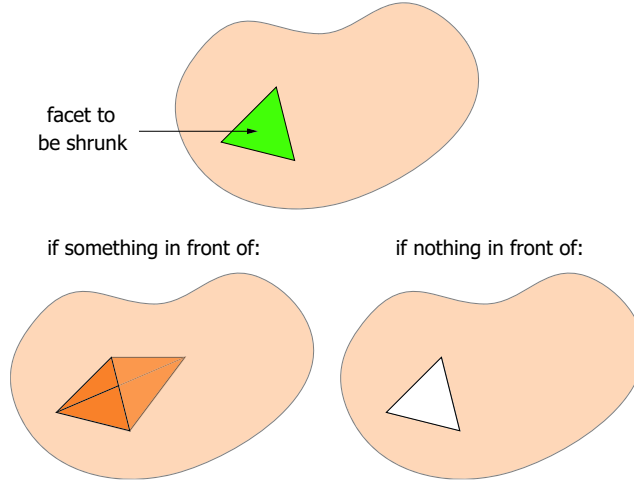

Figure 6: Surface shrunk through a half-facet : two cases depending on whether the hidden tetrahedron is inside or outside the volume delimited by the surface

3.2.1 Algorithm

> **for all** half-facet f of the evolving surface **do**
>> **if** f does not meet the Gabriel property **then**
>>> - deletion of f
>>> **if** it does not cause any local intersection of the evolving surface (at the level of f and its coupled half-facet $\overline{f}$) **then**
>>>> - replacement of f by the 3 half-facets hidden by it
>>> **else**
>>>> - deletion of $\overline{f}$
>>> **end if**
>> **end if**
> **end for**

Fig. 7 illustrates the result of the algorithm in the 2D case. You can notice that the convection result can locally be composed of coupled half-facets that both meet the Gabriel property. We call them *thin parts*.

Figure 7: 2D Convection towards a 2D set of points

Figure 8: Convection towards Bunny point set, with removal of thin parts

3.2.2 Volumic and non-volumic versions of the algorithm

There are two versions of the algorithm according to whether thin parts of the result are kept or not. We usually want to get rid of these non-manifold parts in case of volumic objects (see Fig. 8) but it is necessary to keep them in the case of surfaces with boundaries. Note that, in this case, it could be possible to retrieve a manifold by locally blowing some space in between coupled half-facets.

3.2.3 Comparison with the sculpture algorithm

This algorithm could be seen as a generalization of the sculpture algorithm of Boissonnat [6]. Both approaches are quite different however. In sculpture algorithms, a weight is allocated to each tetrahedron hidden by the evolving surface, so that each step of the algorithm

results in the exudation of the tetrahedron holding the largest weight. The weights chosen must favor the elimination of tetrahedra that lay behind larger, bad-shaped facets. Such an elimination process is run under control of a priority queue and under the constraint of topological genus invariance. The problem is that the order of the facets in the priority queue can be misleading. It does not take care of global data configuration. In some cases, the sculpture process can locally be stopped to respect topological properties (see Fig. 9), while an other elimination sequence could have driven to a better result. Veltkamp pointed out this problem in [14].

Figure 9: Sculpture result : We have added topological constraints and a priority queue to make our algorithm a sculpture algorithm. The weight of a half-facet can be seen as some measure of the Gabriel property. The original shape could not be extracted. This figures out the topological clamping of a sculpture algorithm.

Unlike sculpture algorithms, our method is not based on a global heuristic and does not require a priority queue. The evolution of the triangulated surface is guided by a physical scheme and is not subject to topological conditions : the topological genus of the evolving surface can change several times before the process reaches equilibrium.

3.3   Oriented nature of the aperture condition

In the geometric algorithm of convection presented above, the evolving surface is shrunk through a half-facet if its associated half-ball is not empty. This means that the half-facets included in the result have their associated half-balls empty, but not necessarily their entire diametral ball. This also means that the convection process is locally driven by conditions with regard to the internal skeleton only.

In this section, we study how the convection algorithm evolves if we replace the aperture condition by an orientation-free version of this condition.

3.3.1   2D sets of points

Lemma 5 *In the 2D case of convection towards a 2D set of points, it does not change the result to keep the original aperture condition or to enlarge it to half-edges whose entire diametral disk contains a point.*

Proof.   It is equivalent to prove that each half-edge resulting from the current oriented algorithm has its entire diametral disk empty.

Suppose that $\overset{\frown}{P_i P_j}$ is a half-hedge of the evolving curve (or of the result) whose coupled half-edge $\overset{\frown}{P_j P_i}$ does not meet the Gabriel property (see Fig. 10).

Let P_h be the point hidden by $\overset{\frown}{P_j P_i}$. By construction, the half-facets $\overset{\frown}{P_i P_h}$ and $\overset{\frown}{P_h P_j}$ have been included into the evolving oriented curve at a previous step of the algorithm. One of them should not meet the Gabriel property, so that it could have been shrunk to discover $\overset{\frown}{P_i P_j}$. This is geometrically incompatible with $\overset{\frown}{P_j P_i}$ not meeting the Gabriel property.   □

A consequence of that result is that the evolving curve cannot intersect itself at the level of two coupled half-edges.

3.3.2   Non extension of the result in 3D

A famous result by Amenta and Bern [7] ensures that the global shape of a smooth object surface can be retrieved from a set of points, when these points are an ϵ-sample of the original surface, with $\epsilon < 0.1$. It means that the distance between any point P of the surface and its closest sampled point is less than a proportion $\epsilon < 0.1$ of the distance $lfs(P)$ to the medial axis. Indeed, under this condition, the restricted Delaunay triangulation constitutes a piece-wise linear approximation of the surface, homeomorphic to it. It is composed of Delaunay facets whose dual Voronoi edges intersect the surface ($\epsilon < 0.1$ ensures that the
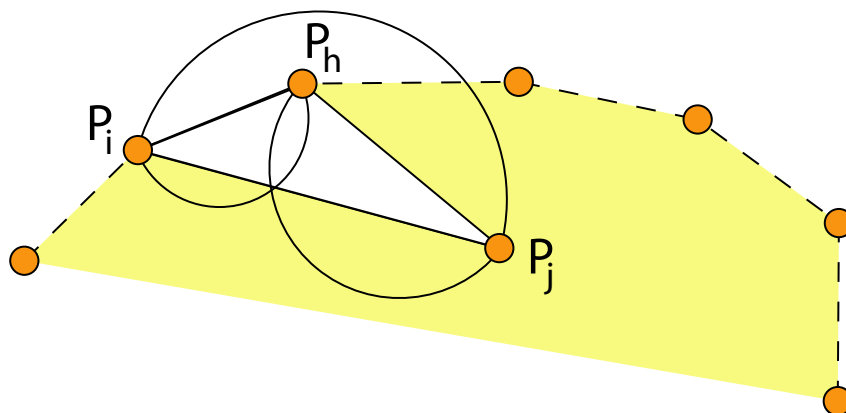
Figure 10: 2D convection property : A discovered half-edge $\overparen{P_i P_j}$ must have its coupled half-facet meeting the Gabriel property, unless it could not have been included into the evolving surface

number of intersections between Voronoi edges and the original surface is less than 1). In practice, it is sometimes impossible to get an ϵ-sample — let us consider, for instance, the case of surfaces that are locally not differentiable — and precise reconstruction of crease edges still remains a problem.

In [15], Petitjean and Boyer have proposed a discrete generalization of the notion of ϵ-sample, to deal with scattered data taken independently of any surface. In this generalization, a set of points is a discrete ϵ-sample if :

- a triangulated surface can be built from it,

- each facet of this triangulation has its size (*granularity*) less than a ratio ϵ of the distance from its vertices to their furthest Voronoi vertices.

Facets of such a triangulation belong to the 3D Delaunay triangulation of the points and they all meet the Gabriel property. Given a discrete ϵ-sample with $\epsilon < 1$, the authors also propose an algorithm which constructs a surface as a set of Gabriel facets in the 3D triangulation of the points.

In practice, sampled sets of points rarely meet the required sampling conditions and the algorithm drawn by Petitjean and Boyer most often produce a surface with boundaries, even when the original surface is unbounded.

It is the case for the "Bunny" point set. To convince ourselves, we ran our algorithm with a different aperture condition on the half-facets : a half-facet is opened if the facet it is supported by is a Gabriel facet. Fig. 11 shows the result of that contraction process after the suppression of the thin parts. As you can see, there was not enough Gabriel facets to stop the progression and the folding up of the surface into itself. This can be a problem if one wishes a closed surface.

Figure 11: Bunny : Opening of half-facets whose entire associated ball contains a point (thin parts are removed). This illustrates the convection result when the oriented nature of the half-facet aperture condition is suppressed.

Why, in practice, are there so much half-facets of the result that meet the Gabriel property but whose associated facet does not itself verify this property ? The point is that the result available in 2D does not extend in 3D, and it is easy to extract configurations of the data where a discovered half-facet has its associated half-ball empty, but not its entire diametral ball.

Let $\overset{\frown}{ABC}$ be a half-facet of the surface. The half-ball associated to $\overset{\frown}{ABC}$ (let us say *in front of* $\overset{\frown}{ABC}$) is empty. The half-ball associated to $\overset{\frown}{BAC}$ (let us say *behind* $\overset{\frown}{ABC}$) can contain a point if the Delaunay tetrahedron $ABCD$ behind $\overset{\frown}{ABC}$ is of the following kind :

- the circumcenter O of $ABCD$ does not lay into the half-plane associated to $\stackrel{\frown}{ADC}$,

- nor into the half-plane associated to $\stackrel{\frown}{BAC}$ (see Fig. 12).

(a) $T = \stackrel{\frown}{ABC}$

(b) *behind T*

Figure 12: In front of and behind a half-facet $T = \stackrel{\frown}{ABC}$

4 Extension of the convection process

Zhao, Osher and Fedkiw used a convection process only to initialize the one of minimizing an energy function. Unfortunately, the convection process can be stuck by the presence of important cavities or pockets exceeding the shape of a cylinder (Fig. 13 illustrates it in 2D).

Let us see how our scheme could be improved in order to solve this issue. If the surface is locally sampled finely enough to detect the presence of the cavity, the distance from points outside the cavity to their neighbors inside the cavity should be bounded by a factor of $lfs(P)$, even if this factor is not always as fine as desired. It means that there should be constraints of consistency between half-facets and local density, even if sampling conditions are not encountered everywhere (at the level of a crease edge, mainly).

Let P be a point of a facet blocking a cavity. If the cavity is sufficiently sampled to be detectable, the distance from P to its surface neighbor, on and outside the cavity, should be small with respect to the blocking facets. Which is clearly not the case, in presence of a cavity (see Fig. 13).

To obtain the results presented in this article, we have made the assumption that the density in the 3D points set is characteristic of the density of the points on the surface.

Figure 13: No digging of cavities exceeding the shape of a cylinder

Consequently, we have improved the aperture condition, so that a half-facet is now opened if its size is not coherent with the local 3D density of the sampling (which is also indicative of the distance to the skeleton). The main problem is to find a good approximation of the density. In practice, we have chosen the distance to the fourth nearest point, keeping in mind that the mean number of neighbors in a 2D triangulation is 6.

5   Topological structure of the result

In the previous sections, we have presented an algorithm that makes an oriented pseudo-surface evolve, subject to topological and geometrical operations. In this section, we are going to describe these operations.

On a triangulated surface of a closed object, each facet lies on 3 different vertices and is adjacent to 3 others facets. Since the vertices of a triangulated surface are geometrically distinct, it is easy to retrieve the connectivity between facets from the geometry of its vertices.

This last remark does not hold for pseudo-surfaces as the ones produced by our algorithm, since different vertices, edges or half-facets can meet common geometric information. The only way to get the connectivity information between half-facets is to store it into a suitable data structure, updated at each step of the convection process, thanks to a set of dedicated operations.

A pseudo-surface is a set of half-facets satisfying the following properties :

- each half-facet is adjacent to 3 others half-facets oriented consistently,

- each half-facet is incident to 3 different vertices,

- two different, non-adjacent vertices can meet a common geometric information.

Such a pseudo-surface is a cellular complex, but not a simplicial complex : two adjacent facets can share more than one common edge. To retrieve an abstract simplicial complex, one barycentric subdivision (such as described by Vegter [16]) is required. After this operation, a half-facet cannot have any longer two equals neighboring half-facets, and each vertex is the center of a topological disk.

5.1 Geometrical and topological operations involved during the convection process

During the convection process, a pseudo-surface evolves such that a half-facet is opened to discover 3 new half-facets adjacent to a new vertex, or such that two coupled half-facets collapse.

It means that the data structure used to represent a pseudo-surface must support the following operations :

- insertion of a new vertex into a half-facet,

- collapse of 2 coupled half-facets (sharing the same geometry but oriented differently).

Vertex insertion is an operation that does not change the topology of the pseudo-surface. As far as the collapse of 2 coupled half-edges is concerned, there are 8 different configurations, depending on the number of common vertices and the number of common edges for the two coupled half-facets. Some of these operations have an effect on the topological structure of the pseudo-surface.

5.1.1   0 common vertex and 0 common edge

- disappearing of 3 vertices,

- disappearing of 3 edges,

- disappearing of 2 half-facets.
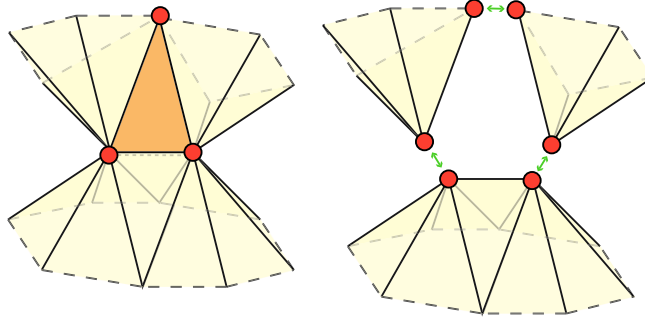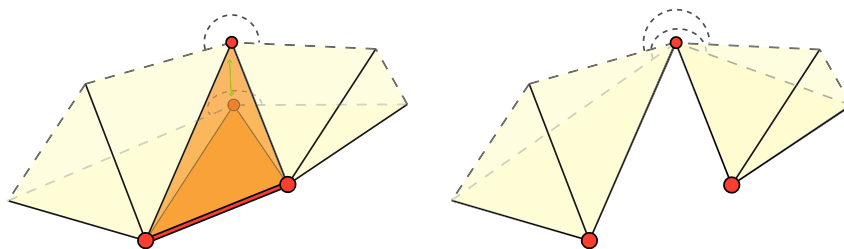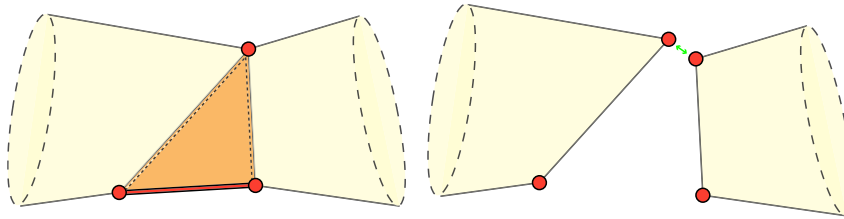

Figure 14: 0 common vertex and 0 common edge

This operation changes the topological structure of the pseudo-surface. It corresponds to a handle creation.

5.1.2   1 common vertex and 0 common edge

- disappearing of 2 vertices and creation of a new vertex,

- disappearing of 3 edges,

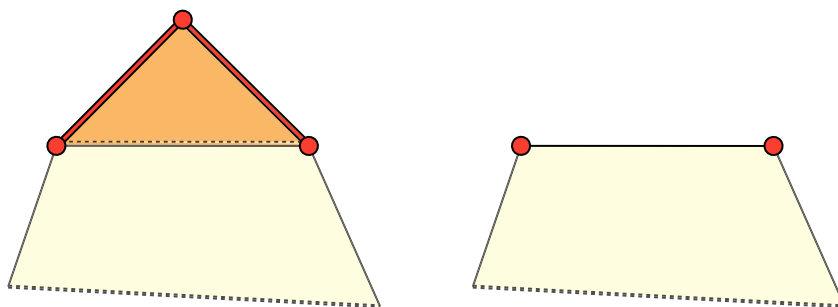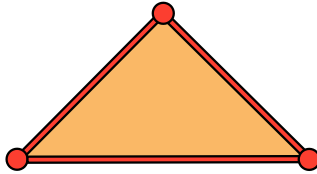- disappearing of 2 half-facets.

Figure 15: 1 common vertex and 0 common edge

This operation does not change the topological structure of the pseudo-surface.

5.1.3   2 common vertices and 0 common edge

- disappearing of a vertex and creation of 2 others,

- disappearing of 3 edges,

- disappearing of 2 half-facets.

Figure 16: 2 common vertices and 0 common edge

This operation changes the topological structure of the pseudo-surface, and that change can be of 2 sorts :

- either a creation of a new connected component,

- either the opening of a handle.

5.1.4 3 common vertices and 0 common edge

- creation of 3 new vertices,

- disappearing of 3 edges,

- disappearing of 2 half-facets.

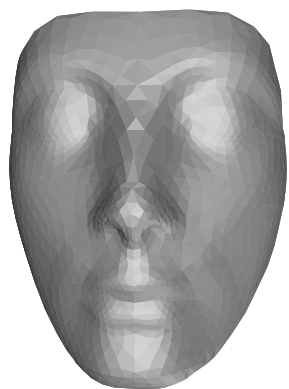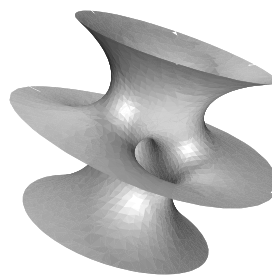Figure 17: 3 common vertices and 0 common edge

This operation changes the topological structure of the pseudo-surface, and that change can be of 4 sorts :

- either a creation of 2 new connected components,

- either the opening of a handle, and the creation of a new connected component,

- either the opening of 2 handles,

- either the opening of 3 handles, and the creation of a new one.

5.1.5   2 common vertices and 1 common edge

- disappearing of 1 vertex,

- disappearing of 3 edges,

- disappearing of 2 half-facets.

Figure 18: 2 common vertices and 1 common edge

This operation does not change the topological structure of the pseudo-surface.

5.1.6   3 common vertices and 1 common edge

- creation of 1 vertex,

- disappearing of 3 edges,

- disappearing of 2 half-facets.

Figure 19: 3 common vertices and 1 common edge

This operation changes the topological structure of the pseudo-surface, with the creation of a new connected component or the opening of a handle.

5.1.7   3 common vertices and 2 common edges

- disappearing of 1 vertex,

- disappearing of 3 edges,

- disappearing of 2 half-facets.

Figure 20: 3 common vertices and 2 common edges

This operation does not change the topological structure of the pseudo-surface.

5.1.8 3 common vertices and 3 common edges

- disappearing of 3 vertices,

- disappearing of 3 edges,

- disappearing of 2 half-facets.

Figure 21: 3 common vertices

This operation changes the topological structure of the pseudo-surface, with the disappearing of a connected component.

6 Results

An implementation of the convection algorithm has been done using CGAL [17]. All the results presented here have been obtained in a few seconds on a Pentium III 850 MHz with 512 MB of RAM.

(a) "Nefertiti" (surface with boundary) 1128 points

(b) "Mathematical surface" (surface with boundary) 6752 points

Figure 22: "Nefertiti" and "Mathematical surface"

Figure 23: "Plane Engine" (surface with boundary) 11444 points

(a) "Schale" (surface with boundary) 2714 points

(b) "Triceratops" (surface without boundaries) 2833 points

Figure 24: "Schale" and "Triceratops"

Figure 25: "Meca" (surface without boundaries) 12594 points

Figure 26: "Fish" (surface with thin parts) 54811 points

7   Conclusion

In this paper, we have dealt with an existing physical convection scheme, that we have translated into a geometric algorithm. This approach seems interesting to us, both to fasten the usual discretizations processes and to extract the possible geometric structure

underlying in an evolution equation. This geometric algorithm is widely based on the 3D Delaunay triangulation of the points, but this latter does not need to be constructed : not all the Delaunay facets are explored and a convex hull algorithm coupled with a location structure can be enough to determine local density at a point and to determine if a half-facet encounters the Gabriel property or not. Current results of the algorithm could also be improved with a better approximation of points density on the surface.

References

[1] H. Hoppe, T. DeRose, T. Duchamp, J. McDonald, and W. Stuetzle. Surface reconstruction from unorganized points. *Comput. Graphics*, 26(2):71–78, 1992. Proc. SIGGRAPH '92.

[2] B. Curless and M. Levoy. A volumetric method for building complex models from range images. In *Proc. SIGGRAPH 96*, pages 303–312, 1996.

[3] F. Bernardini, C. Bajaj, J. Chen, and D. Schikore. Triangulation-based object reconstruction methods. In *Proc. 13th Annu. ACM Sympos. Comput. Geom.*, pages 481–484, 1997.

[4] M. Gopi, S. Krishnan, and C. T. Silva. Surface reconstruction based on lower dimensional localized Delaunay triangulation. In *Eurographics*, 2000.

[5] H. Edelsbrunner, D. G. Kirkpatrick, and R. Seidel. On the shape of a set of points in the plane. *IEEE Trans. Inform. Theory*, IT-29:551–559, 1983.

[6] Jean-Daniel Boissonnat. Geometric structures for three-dimensional shape representation. *ACM Trans. Graph.*, 3(4):266–286, 1984.

[7] Nina Amenta and Marshall Bern. Surface reconstruction by Voronoi filtering. *Discrete Comput. Geom.*, 22(4):481–504, 1999.

[8] N. Amenta, S. Choi, T. K. Dey, and N. Leekha. A simple algorithm for homeomorphic surface reconstruction. In *Proc. 16th Annu. ACM Sympos. Comput. Geom.*, pages 213–222, 2000.

[9] N. Amenta, S. Choi, and R. K. Kolluri. The power crust, unions of balls, and the medial axis transform. *Comput. Geom. Theory Appl.*, 19:127–153, 2001.

[10] Jean-Daniel Boissonnat and Frédéric Cazals. Smooth surface reconstruction via natural neighbour interpolation of distance functions. In *Proc. 16th Annu. ACM Sympos. Comput. Geom.*, pages 223–232, 2000.

[11] Joachim Giesen and Matthias John. Surface reconstruction based on a dynamical system. In *Proc. Eurographics*, 2002.

[12] Herbert Edelsbrunner. Surface reconstruction by wrapping finite sets in space. Technical report, to appear in Ricky Pollack and Eli Goodman Festschrift, ed. B. Aronov, S. Basu, J. Pach and M. Sharir, Springer-Verlag, 2002.

[13] H.K.Zhao, S. Osher, and R. Fedkiw. Fast surface reconstruction using the level set method. In *Proceedings of IEEE Workshop on Variational and Level Set Methods in Computer Vision (VLSM)*, 2001.

[14] Remco C. Veltkamp. Boundaries through scattered points of unknown density. *Graphical Models and Image Processing*, 57(6):441–452, 1995.

[15] Sylvain Petitjean and Edmond Boyer. Regular and non-regular point sets : properties and reconstruction. *Computational Geometry : Theory and applications - Elsevier*, 19(2-3):101–126, 2001.

[16] Gert Vegter. *Handbook of Discrete and Computational Geometry - J.E. Goodman and J. O'Rourke eds*, chapter 28 - Computational topology, pages 517–536. CRC Press LLC, Boca Raton, Florida, 1997.

[17] *http://www.cgal.org*.

Contents